Pre-Clinical Testing of a Novel Thin Film Nitinol Flow Diversion Stent in a Rabbit Elastase Aneurysm Model

YongHong Ding[1,*], **Daying Dai**[1], **David F. Kallmes**[1], **Dana Schroeder**[1], **Colin P. Kealey**[2], **Vikas Gupta**[2], **A. David Johnson**[2], and **Ramanathan Kadirvel**[1]

[1]Mayo Clinic, Department of Neurointerventional Radiology, Rochester, Minnesota

[2]NeuroSigma, Inc., Los Angeles, California

Abstract

Purpose—Thin Film Nitinol (TFN) can be processed to produce a thin microporous sheet with low percent metal coverage (<20%) and high pore density (~70 pores/mm^2) for flow diversion. We present in vivo results from treatment of experimental rabbit aneurysms using a TFN-based flow diversion device.

Materials and Methods—Nineteen aneurysms in the rabbit elastase aneurysm model were treated with a single TFN flow diverter. Devices were also placed over 17 lumbar arteries to model peri-aneurysmal branch arteries of the intracranial circulation. Angiography was performed at 2 weeks (n=7), 1 month (n=8) and 3 months (n=4) immediately before sacrifice. Aneurysm occlusion was graded on a 3-point scale (Grade 1, complete occlusion; Grade 2, near-complete occlusion; Grade 3, incomplete occlusion). Toluidine blue staining was used for histologic evaluation. En face CD31 immunofluorescent staining was performed to quantify neck endothelialization.

Results—Markedly reduced intra-aneurysmal flow was observed on angiography immediately after device placement in all aneurysms. Grade 1 or 2 occlusion was noted in four (57%) aneurysms at 2-week, in six (75%) aneurysms at 4-week and in three (75%) aneurysms at 12-week follow-up. All 17 lumbar arteries were patent. CD31 staining showed that $75 \pm 16\%$ of the aneurysm neck region was endothelialized. Histopathology demonstrated incorporation of the TFN flow diverter into the vessel wall and no evidence of excessive neointimal hyperplasia.

Conclusion—In this rabbit model, the TFN flow diverter achieved high rates of aneurysm occlusion and promoted tissue in-growth and aneurysm neck healing, even early after implantation.

Introduction

Flow diverters (FDs) are a relatively recent advancement in the endovascular treatment of intracranial aneurysms (IAs) and have expanded the types of aneurysms addressable with endovascular techniques (1–5). Numerous different flow diverters have been approved in

*Address reprint requests to Yonghong Ding, MD, Department of Radiology, Mayo Clinic, 200 First St SW, Rochester, MN, 55905; ding.yonghong@mayo.edu. Telephone: 507-266-3350. Fax: 507-255-0706.

Europe, and several are either approved for use or under investigation in the U.S. Each of the flow diversion devices in current use is constructed from braided metallic strands, typically nitinol, cobalt chromium, and/or platinum. These devices, while promising, suffer from several relative disadvantages. Aneurysm occlusion may be delayed, precise placement may be challenging because of device shortening, more than one device is often required, and branch arteries covered by the device may undergo occlusion (6–8).

Thin film nitinol (TFN) is a biomaterial produced in patterned sheets approximately 5 μm thick using techniques adapted from the microelectronics industry. Previous reports have demonstrated that TFN has unique mechanical properties, excellent biocompatibility, and a low profile that make it well suited for use in endovascular devices (9–11). Potential advantages of a flow diverting stent based on TFN technology include the ability to fabricate devices with significantly higher pore densities and a lower percent metal coverage than is achieved with current generation devices based on braided wire technology. The purpose of this study was to test a novel TFN-based flow diverting stent in a rabbit model of saccular aneurysms.

Materials and Methods

Aneurysms (n=19) were created in New Zealand white rabbits. Our Institutional Animal Care and Use Committee approved all animal procedures. Detailed procedure for aneurysm creation has been described previously (12). Briefly, anesthesia was induced with an intramuscular injection of ketamine (35 mg/kg), xylazine (6 mg/kg), and acepromazine (1.0 mg/kg), and maintained with 2.5–3.0% isoflurane conveyed in 100% oxygen. Using a sterile technique, we exposed and ligated the RCCA distally. A 1- to 2-mm bevelled arteriotomy was made and a 5F vascular sheath (Cordis Endovascular, Miami Lakes, FL) was advanced retrogradely in the RCCA to a point approximately 3 cm cephalad to the origin of RCCA. Fluoroscopy (Advantx; GE Healthcare, Milwaukee, Wisconsin) was performed by injection of contrast through the sheath retrogradely in the RCCA, to identify the junction between the RCCA and the subclavian and brachiocephalic arteries. A 3F Fogarty balloon (Baxter Healthcare, Irvine, California) was advanced through the sheath to the level of the origin of the RCCA with fluoroscopic guidance and was inflated with iodinated contrast material. Porcine elastase (5.23 μ/mgP, 40.1 mgP/mL, approximately 200 U/mL; Worthington Biochemical, Lakewood, New Jersey) was incubated within the lumen of the common carotid artery above the inflated balloon for 20 minutes, after which the catheter, balloon, and sheath were removed and the RCCA was ligated below the sheath entry site.

Three weeks after creation, patency of all the aneurysms and parent arteries were confirmed by DSA before TFN device deployment. A 5 French sheath was advanced in one side of femoral artery via cutdown, followed by 5 French Envoy guiding catheter (Cordis Neurovascular, Miami Lakes, FL). A distal access catheter with .044 inch ID (Concentric Medical, Mountain View, CA) was advanced into the distal end of parent artery (right subclavian artery, RSCA) over a .038 inch guidewire with hydrophilic coating (Boston Scientific Corporation, Natick, MA) through the guide catheter.

Prototype TFN flow diverters were fabricated and provided for this study by NeuroSigma, Inc. (Los Angeles, CA). Detailed methods for the fabrication of TFN have been published previously (13–15). In brief, TFN is sputter deposited on four-inch silicon wafers using a custom DC magnetron sputter system. Silicon wafers are micropatterned using Deep Reactive Ion Etching (DRIE) prior to the sputter deposition process. Following deposition, the TFN is removed from the silicon wafer and annealed at 500° C. This process yields a cylindrical TFN micromesh that is subsequently used to cover a laser-cut nitinol backbone stent (Figure 1). The red box outlines an area of 1 mm^2. The pore density and percent metal coverage of the TFN flow diverter were calculated from SEM images of a device at full expansion. The number of pores in an area of 1mm^2 was counted from the SEM image and percent metal coverage was calculated from the following formula: (1 - Percent Metal Coverage of Stent Backbone). At full expansion, the TFN flow diverter had a pore density of approximately 70 pores/mm^2 and a percent metal coverage of less than 20%. Results from in vitro and in vivo testing of devices constructed using similar methods have been reported previously (9–11).

The first TFN device (4.5 mm OD × 12 mm) was deployed across the aneurysm neck by pushing the device out of the distal access catheter with the .038 inch guidewire with hydrophilic coating. The second device (4.5mm OD × 12 mm) was deployed across a lumbar artery within the abdominal aorta. DSA was performed through the guide catheter immediately after deployment. No damage of the device occurred during deployment. Aspirin (10 mg/kg) and Clopidogrel (10 mg/kg) were given daily 2 days before implantation and continued till 30 days after treatment.

Sacrifice was performed at 2 weeks (n = 7), 4 weeks (n = 8), and 12 weeks (n = 4) after treatment. On the day of sacrifice, anesthesia was administered as a cocktail of ketamine (74 mg/kg), xylazine (5 mg/kg) and acepromazine (1mg/kg). Surgical access of the left CFA was achieved. DSA was performed for both brachiocephalic trunk and abdominal aorta. Degree of aneurysm occlusion immediately after device deployment and before sacrifice were graded on a 3-point scale based on DSA images, including Grade 1 (complete flow cessation, no flow within the aneurysm), Grade 2 (near complete flow, <10% residual flow), Grade 3 (incomplete occlusion, 10% residual flow) (13). Patency of the parent artery and lumbar artery (including stenosis or occlusion) were assessed from DSA. Immediately following angiography, the subjects were euthanized using a lethal injection of pentobarbital. The aneurysm, stented parent artery and the aorta were harvested and fixed in 10% formalin. Toluidine blue staining was performed to evaluate thrombus organization within aneurysm and neointima coverage of aneurysm neck and the orifice of lumbar artery.

Gross pathology and *en face* CD31 immunofluorescent staining was performed on a subset of devices selected at random from each of the follow-up time points to quantify neck endothelialization (n=1 at 2 weeks, n=3 at 4 weeks, and n=2 at 12 weeks). Whole mount immunofluorescent staining was performed using anti-CD31 antibody. The coverage percentage of endothelialized neointima across the neck was calculated by using the value of neck area of endothelialization measured under microscope and the whole neck area. Histopathology of explanted devices was performed on one device at each of the three time points using plastic section mounting and toluidine blue staining.

Results

Mean aneurysm sizes (including aneurysm neck, width, and height), and angiographic outcomes from the 19 aneurysms are shown in Table 1.

Grades 1 or 2 occlusion rates were noted in 57% (n=4) aneurysms at the 2-week follow-up time point (Figure 2A–C). At the 4-week time point, six (75%) aneurysms had complete or near complete occlusion (Grades 1 or 2) (Figure 3A–C). At the 12-week time point, three (75%) aneurysms showed Grades 1 or 2 aneurysm occlusion. Distal parent artery was occluded in one aneurysm immediately after device deployment but reopened at the 3-month follow-up time point. Overall, grades 1 or 2 occlusion rates were achieved in 13 (68%) of the 19 aneurysms. All other parent arteries and lumbar arteries remained patent without stenosis (Figure 2E–G and 3 E–G).

Gross pathology along with en face CD 31 immunofluorescent staining, showing 89% of aneurysm neck area was covered by endothelialized tissue (area 1, 2 and 3). E. DSA image showing lumbar arteries before deployment in abdominal aorta (striped right arrow). F. DSA image immediately after device deployment, showing patent lumbar arteries (striped right arrow). G. DSA image at 4 weeks of deployment, showing that lumbar arteries remain patent (striped right arrow).

For the six aneurysms with histology processing, the average implant duration was 6.3 weeks. The mean neck orifice area was 6.3 ± 2.5 mm^2, $75 \pm 16\%$ of the aneurysm neck region was covered by endothelialized tissue at the time of sacrifice (Figure 2D and 3 D). Toluidine blue staining of aneurysms with explanted devices confirmed these findings, which included minimal neointimal hyperplasia and good incorporation of the TFN and support stent. Thrombus formation within aneurysm was also indicated (Figure 4).

Discussion

In this study, we demonstrated that a single TFN flow diverter could achieve high rates of complete or near complete aneurysm occlusion as early as two weeks after implantation. Further, rapid and near-complete endothelialization was noted across aneurysm necks, while branch arteries remained patent in all cases. All these results offer evidence that the TFN flow diverter holds substantial promise for clinical use.

Numerous flow diverting devices have previously been tested in the elastase aneurysm model and subsequently been applied clinically (16–22). Aneurysm occlusion, neointimal hyperplasia of parent artery (stenosis or occlusion), distal parent artery emboli, and patency of branch artery all can be assessed in this aneurysm model. As compared to current flow diverter devices, the NeuroSigma TFN flow diverter achieves a very high pore density while, at the same time, allowing low percent metal coverage. This feature gave very small distances needed for endothelial cells to cross between structural elements of the TFN.

This study has several limitations. The number of subjects at each time point was relatively small, and the duration of implantation was limited. The aneurysms in this study were small even though the mean height of aneurysm was around 10 millimeters. The longest time point

for follow-up was only 3 months in this study. Finally, the morphology of the aneurysms does not provide the range to be expected clinically, and the tortuosity of the carotid siphon and other vessel territories in humans may cause substantial challenges in achieving adequate wall apposition of the device.

Conclusion

In this rabbit model the TEN devices achieved high rates of acute angiographic occlusion. Vessel branches covered by the devices remained patent. High degrees of endothelialization across aneurysm neck were achieved which indicates that, in this model, the TEN can promote tissue ingrowth and aneurysm neck healing.

Acknowledgments

References

1. Kallmes DF, Hanel R, Lopes D, et al. International Retrospective Study of the Pipeline Embolization Device: A Multicenter Aneurysm Treatment Study. AJNR Am J Neuroradiol. 2015; 36:108–15. [PubMed: 25355814]

2. Saatci I, Yavuz K, Ozer C, et al. Treatment of Intracranial Aneurysms Using the Pipeline Flow-Diverter Embolization Device: A Single-Center Experience with Long-Term Follow-Up Results. AJNR Am J Neuroradiol. 2012; 33:1436–46. [PubMed: 22821921]

3. Berge J, Biondi A, Machi P, et al. Flow-Diverter Silk Stent for the Treatment of Intracranial Aneurysms: 1-year Follow-Up in a Multicenter Study. AJNR Am J Neuroradiol. 2012; 33:1150–55. [PubMed: 22300924]

4. Lubicz B, Elst O, Collignon L, et al. Silk Flow-Diverter Stent for the Treatment of Intracranial Aneurysms: A Series of 58 Patients with Emphasis on Long-Term Results. AJNR Am J Neuroradiol. 2015; 36:542–46. [PubMed: 25376806]

5. Briganti F, Leone G, Marseglia M, Cicala D, Caranci F, Maiuri F. p64 Flow Modulation Device in the treatment of intracranial aneurysms: initial experience and technical aspects. J Neurointerv Surg. 10.1136/neurintsurg-2015-011743

6. Tan LA, Keigher KM, Munich SA, et al. Thromboembolic complications with Pipeline embolization device placement: impact of procedure time, number of stents and pre-procedure P2Y12 reaction unit (PRU) value. J NeuroIntervent Surg. 10.1136/neurintsurg-2014-011111

7. Cirillo L, Leonardi M, Dall'olio M, et al. Complications in the treatment of intracranial aneurysms with Silk stents: an analysis of 30 consecutive patients. Interv Neuroradiol. 2012; 18:413–25. [PubMed: 23217636]

8. Vries JD, Boogaarts J, Norden AV, et al. New generation of flow diverter (Surpass) for unruptured intracranial aneurysms: a prospective single-center study in 37 patients. Stroke. 2013; 44:1567–77. [PubMed: 23686973]

9. Shayan M, Chun Y. An overview of thin film nitinol endovascular devices. Acta Biomater. pii: S1742–7061(15)00135-X.

10. Kealey CP, Chun YJ, Viñuela FE, et al. In vitro and in vivo testing of a novel, hyperelastic thin film nitinol flow diversion stent. J Biomed Mater Res B Appl Biomater. 2012; 100:718–25. [PubMed: 22121079]

11. Kealey CP, Whelan SA, Chun YJ, et al. In vitro hemocompatibility of thin film nitinol in stenotic flow conditions. Biomaterials. 2010; 31:8864–71. [PubMed: 20810163]

12. Ding YH, Dai D, Kadirvel R, Lewis DA, Kallmes DF. Five-year follow-up in elastase-induced aneurysms in rabbits. AJNR Am J Neuroradiol. 2010; 31:1236–39. [PubMed: 20223890]

13. Gupta, V.; Johnson, AD.; Martynov, V.; Menchaca, L. Nitinol thin film three-dimensional devices: fabrication and applications. In: Pelton, AR.; Duerig, T., editors. SMST-2003: Proceedings of the International Conference on Shape Memory and Superelastic Technologies. SMST Society Inc; 2004. p. 639-650.

14. Mohanchandra KP, Ho KK, Carman GP. Compositional uniformity in sputter-deposited NiTi shape memory alloy thin films. Materials Letters. 2008; 62:3481–3483.

15. Chun YJ, Levi DS, Mohanchandra KP, et al. Novel micro-patterning processes for thin film NiTi vascular devices. Smart Materials and Structures. 2010; 19:105021.

16. Brinjikji W, Lanzino G, Cloft HJ, Kallmes DF. Patency of the posterior communicating artery after flow diversion treatment of internal carotid artery aneurysms. Clinical Neurology and Neurosurgery. 2014; 120:84–8. [PubMed: 24731582]

17. Kallmes DF, Ding YH, Dai D, et al. A new endoluminal, flow-disrupting device for treatment of saccular aneurysms. Stroke. 2007; 38:2346–52. [PubMed: 17615366]

18. Kallmes DF, Ding YH, Dai D, et al. A second-generation, endoluminal, flow-disrupting device for treatment of saccular aneurysms. AJNR Am J Neuroradiol. 2009; 30:1153–58. [PubMed: 19369609]

19. Simgen A, Ley D, Roth C, et al. Evaluation of a newly designed flow diverter for the treatment of intracranial aneurysms in an elastase-induced aneurysm model, in New Zealand white rabbits. Neuroradiology. 2014; 56:129–37. [PubMed: 24496551]

20. Struffert T, Ott S, Kowarschik M, et al. Measurement of quantifiable parameters by time-density curves in the elastase-induced aneurysm model: first results in the comparison of a flow diverter and a conventional aneurysm stent. Eur Radiol. 2013; 23:521–7. [PubMed: 22895618]

21. Ionita CN, Natarajan SK, Wang W, et al. Evaluation of a second-generation self-expanding variable-porosity flow diverter in a rabbit elastase aneurysm model. AJNR Am J Neuroradiol. 2011; 32:1399–407. [PubMed: 21757527]

22. Sadasivan C, Cesar L, Seong J, et al. An original flow diversion device for the treatment of intracranial aneurysms: evaluation in the rabbit elastase-induced model. Stroke. 2009; 40:952–58. [PubMed: 19150864]
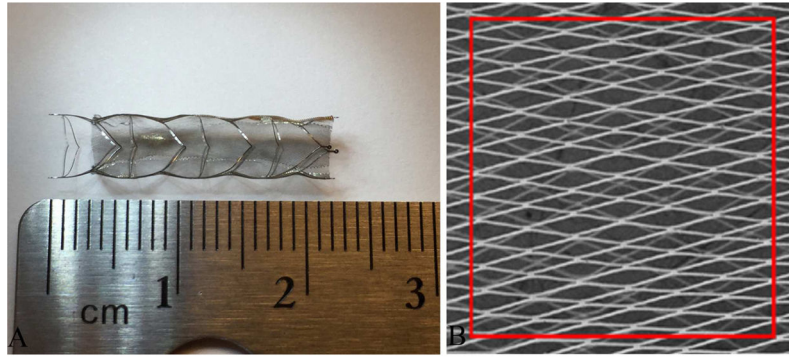
Figure 1.
Figure 1A, showing a prototype TFN flow diverter; 1B, showing the scanning electron microscopy image of TFN.
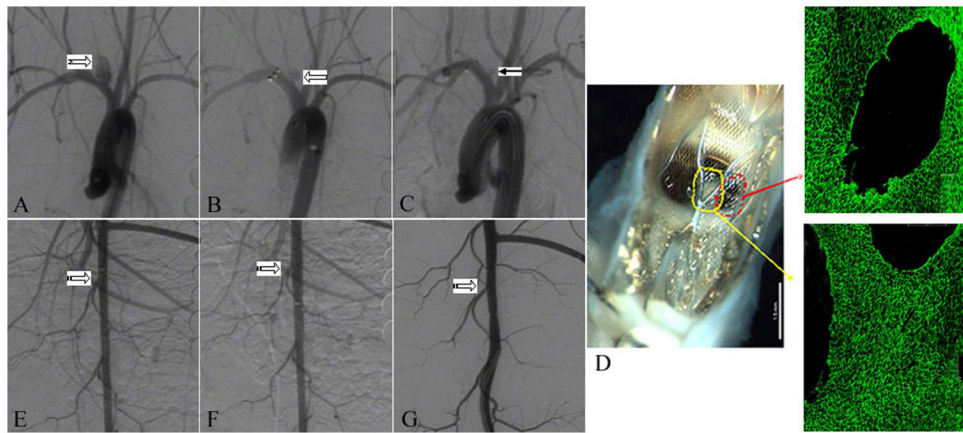
Figure 2.
A. Digital subtraction angiogram (DSA) showing aneurysm before treatment (notched right arrow). B. DSA image immediately after device deployment, showing blood flow reduction in the aneurysm (left block arrow). C. DSA image at 2 weeks of deployment, showing near-complete aneurysm occlusion (Grade 2) (left arrow). D. Gross pathology along with en face CD 31 immunofluorescent staining, showing 46% of aneurysm neck area was covered by endothelialized tissue (red and yellow arrow). E. DSA image showing lumbar arteries before deployment in abdominal aorta (striped right arrow). F. DSA image immediately after device deployment, showing patent lumbar arteries (striped right arrow). G. DSA image at 2 weeks of deployment, showing that lumbar arteries remain patent (striped right arrow).
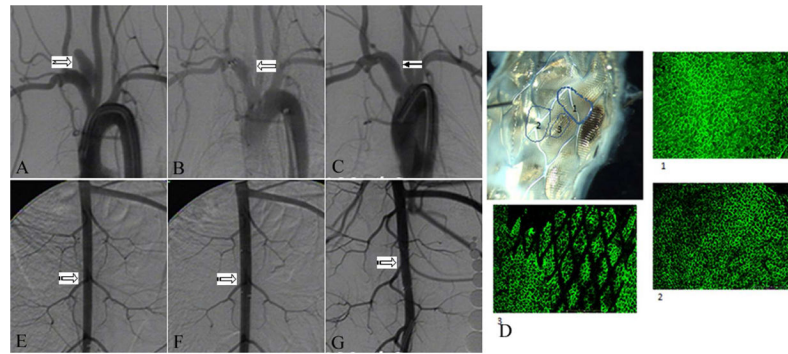
Figure 3.
A. Digital subtraction angiogram (DSA) showing aneurysm before treatment (notched right arrow). B. DSA image immediately after device deployment, showing significant blood flow reduction in the aneurysm (left block arrow). C. DSA image at 4 weeks of deployment, showing complete aneurysm occlusion (Grade 1) (left arrow). D.
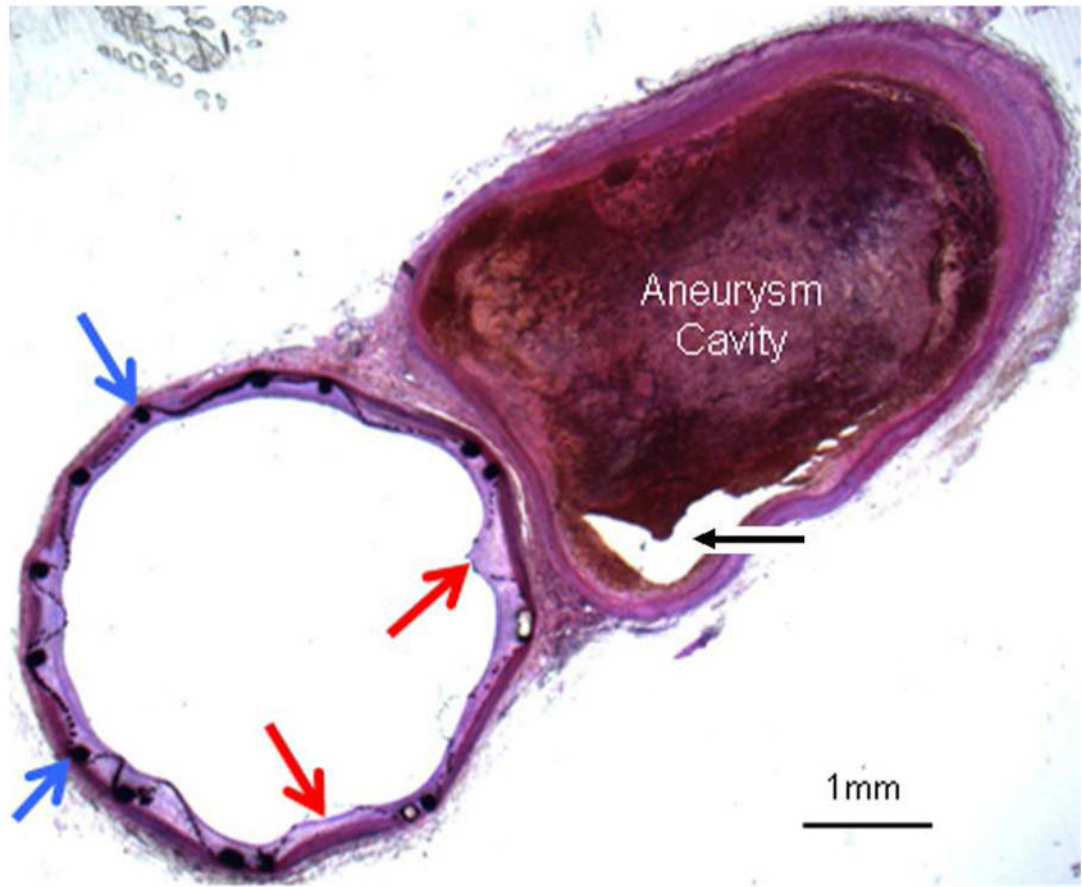
Figure 4.
Histologic section (toluidine blue staining) of TFN flow diverter explanted after 4 weeks.
This axial image demonstrates minimal neointimal hyperplasia deep to the TFN (red arrows)
and support stent (blue arrows). Aneurysm cavity is partially filled with thrombus in various
stages of organization. A small part of the aneurysm lumen is empty (black arrow).

Table 1

Aneurysm Size and Angiographic Outcome

| Time Point (Weeks) | Mean Aneurysm Size (mm) | | | Occlusion Grades | | Lumbar Artery Patency (%) |
	Neck	Width	Height	Grade 1 or 2	Grade 3	
2	4.0 ± 1.4	4.5 ± 1.5	9.8 ± 2.4	57%	43%	100
4	4.1 ± 1.0	4.1 ± 1.4	9.3 ± 1.6	75%	25%	100
12	4.1 ± 1.0	4.7 ± 2.1	9.5 ± 2.7	75%	25%	100